•TECHNOLOGY•RESEARCH•HIGHLIGHTS•VISIONS•SCIENCE
128

The effect of geometry on radionuclide transport in a bedrock fracture

Karita Kajanto

VTT TECHNOLOGY 128

The effect of geometry on radionuclide transport in a bedrock fracture

Karita Kajanto

ISBN 978-951-38-8055-2 (URL: http://www.vtt.fi/publications/index.jsp)

VTT Technology 128

ISSN-L 2242-1211
ISSN 2242-122X (Online)

JULKAISIJA – UTGIVARE – PUBLISHER

VTT
PL 1000 (Tekniikantie 4 A, Espoo)
02044 VTT
Puh. 020 722 111, faksi 020 722 7001

VTT
PB 1000 (Teknikvägen 4 A, Esbo)
FI-02044 VTT
Tfn +358 20 722 111, telefax +358 20 722 7001

VTT Technical Research Centre of Finland
P.O. Box 1000 (Tekniikantie 4 A, Espoo)
FI-02044 VTT, Finland
Tel. +358 20 722 111, fax + 358 20 722 7001

The effect of geometry on radionuclide transport in a bedrock fracture

Karita Kajanto. Espoo 2013. VTT Technology 128. 29 p.

Abstract

a) Background b) What should be done? c) Methods and tool

a) Estimating the long term safety of a geological nuclear waste repository is a complicated computational problem. Numerous scenarios of system failure must be taken into account. Released radionuclides can be transported long distances along the groundwater of rock fractures. Sorption into the bedrock may also take place. In the case of a release of radionuclides to the groundwater, transport properties in fractures must be well known. A common approximation of rock fracture flow is flow between parallel plates. The shape of natural fractures, however, is uneven and irregular. Varying shape and size causes dispersion that affects transport.

b) Study the effect of dispersion caused by variable aperture fractures to the transport and flow properties. Build models of a single rock fracture in different credible geometries. Calculate the flow field and transport of a pulse of radionuclides trough the fractures. Also, calculate the retention of nuclides caused by matrix diffusion. Compare the results to the parallelplate case.

c) Numerical methods: FEM with time integration. COMSOL Multiphysics 4.2a, CAD Import Module, Subsurface Flow Module, Chemical Reaction Engineering Module.

Keywords radionuclide transport, bedrock fracture, matrix diffusion, parallel plate approximation

Preface

This special assignment was carried out in the Nuclear Waste Management Team of VTT during the spring of 2012. I would like to thank my colleagues at VTT for their help and ideas.

Contents

1 Introduction

The exploitation of nuclear power produces highly radioactive waste. After considerations, final disposal into geosphere and complete isolation from biosphere has been chosen as the primary plan of operation for the spent fuel. Many other possible placements for the storage have been proposed, for example deep sea, space and glaciers [1]. Each of these alternatives present difficulties, especially ethical. Another approach to handle the radioactive waste is transmutation, the nuclear modification of spent fuel. The most long-living nuclides would be separated and modified to be less harmful. The technology is not yet complete, research in the field is done and economical uncertainties are still significant [2]. This alternative is mainly considered in countries that use nuclear power extensively, for example France.

Finland and several other small nuclear countries have chosen geological disposal as their method to dispose of nuclear waste. As the fuel is highly radioactive for a significant amount of time, special care must be taken when planning the isolation of the system. Finland is following the plan KBS-3, wherein the waste is placed into solid bedrock in durable canisters. KBS-3 is a radioactive waste disposal concept originally developed in Sweden [3]. The concept consists of several steps. After a cooling period, the fuel rods are placed in cast iron inserts, which are encapsulated in copper canisters. The containers are placed in crystalline bedrock 400-500 m underground and surrounded with a layer of bentonite clay. The full storage will be sealed and the tunnels filled. After approximately 250 000 years the activity of the waste has reduced down to the activity of a large uranium ore body, and can be considered harmless [4].

Nuclear waste containers are placed in a depth of several hundreds of meters, which is well below the groundwater surface. In this depth, groundwater is the only route of access to the containers. Water transmits corrosive substances, and after a leak out of the container, water can transport radionuclides for long distances. This is why the primary goal of the multiple barriers around the fuel rods is to delay and limit the contact of the fuel rods with water and thus limit the spreading of radionuclides. The safety of this system is based on the premise that each component of the system functions independently [3, 5].

The copper canister is very resistant to corrosion, and the operating life expectancy for a flawless canister is 100 000 years at least [4]. Much research is done to the understanding of the behaviour of bentonite buffer [6]. The buffer has multiple tasks, for example limiting the flow of water and thus reducing transport mechanisms of radionuclides to diffusion only. It helps maintaining optimal chemical and thermal conditions and limits microbiological processes. Bentonite clay also cushions the container against mechanical stresses, such as movements of the bedrock.

Safety assessment is a method to estimate radionuclide releases into the biosphere. In safety assessment also unlikely scenarios must be taken into account. It is assumed that eventually radionuclides will escape despite the barriers, following the conservative principle to choose an alternative that overestimates the radiological effects. The escape can take place sooner, due to a manufacturing defect in the copper canister, or later due to corrosion. Even though the mechanism which leads to the failure of the canister might be unclear, the safety of such a case must be evaluated. Radionuclides will in time find their way to bedrock and dilute into the groundwater.

Crystalline bedrock has a network of fractures, where the groundwater flows. Once nuclides have escaped the barriers, they can be transported significant distances through these fractures, dissolved into the groundwater [4, 7, 8]. On their way through the bedrock, escaped radionuclides may diffuse into the porous rock and react, depending on the chemical species of the nuclide and the geochemical properties of the rock. Some substances may attach chemically on mineral surfaces for longer periods, which leads to the retention of the nuclide. The understanding of these transport and retention phenomena is essential to safety assessment calculations.

A lot of work has been done in the field of transport modelling in fractures and fracture networks [9, 10]. Complex simulations of fracture networks, often semi-synthetic, have been run and studied [4, 7, 8]. The work is roughly divided into site characterization and performance assessment, which differ vastly. Typical for performance assessment are very large and simplified geometries and averaging of the heterogeneous properties over large volumes. Site characterization on the other concentrates on describing the site accurately, with immense amount of detail and heterogeneity.

The aim of this assignment is to examine the validity of the assumption that fractures in bedrock can be assumed to be smooth in calculations. In real fractures the aperture size and shape varies. The changing aperture causes dispersion due to the varying velocity field [9]. In the simplest, fracture transport can be calculated with constant flow between parallel plates with molecular diffusion only in the direction perpendicular to the fracture, into the rock matrix. This approach eliminates all sources of dispersion. In this work, the variable aperture as a source of dispersion is studied.

Different synthetic fractures with variable aperture are created (figure 1), and transport of a radionuclide pulse through them is examined in respect to parallel plates. The flow field of water is solved with Navier-Stokes equations and diffusion is assumed isotropic in both synthetic and smooth fractures.

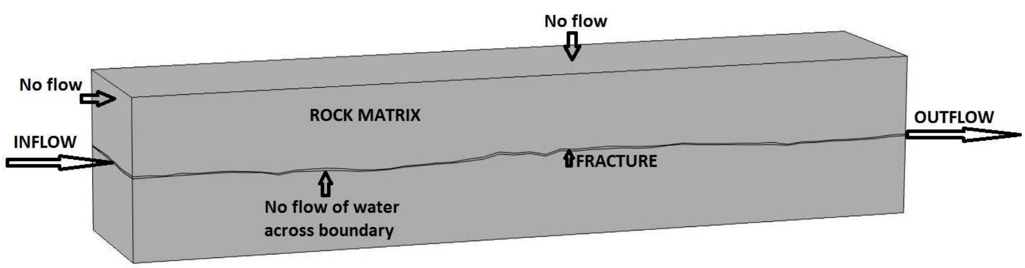

Figure 1: Schematic picture of the system. Outer boundaries of the rock domains are assumed impermeable, internal boundaries hold a no-flow condition for water, but allow diffusion of nuclides into the rock matrix.

2 Theory

The physical phenomena taken into account here are the flow of groundwater and the transport of radionuclides. Temperature effects are ignored, and chemical reactions are included only indirectly. The basic problem is to calculate the flow field in the fracture and then transport of the dissolved matter in both fracture and bedrock.

2.1 Navier-Stokes equations

The equations describing fluid flow are the Navier-Stokes equations. They can be derived by applying Newtons second law to fluid dynamics [11]. In general form the equations are the conservation of momentum

$$\rho\left(\frac{\partial \mathbf{u}}{\partial t} + \mathbf{u}\cdot\nabla\mathbf{u}\right) = -\nabla p + \nabla\cdot\mathbb{T} + \mathbf{F}, \tag{1}$$

and the continuity equation

$$\frac{\partial \rho}{\partial t} + \nabla\cdot(\rho\mathbf{u}) = 0. \tag{2}$$

In these equations $\mathbf{u}$ is the fluid velocity, ρ density, p pressure, $\mathbb{T}$ the viscous stress tensor and $\mathbf{F}$ contains the body forces.

In fracture flow a number of assumptions can be made. Fluid is assumed to be firstly Newtonian and secondly incompressible. The assumption of incompressibility is not obvious, but the pressure differences are small in the examined cases and there are no temperature gradients. Thus the density can be considered to remain constant.

A Newtonian fluid has a linear stress versus strain rate curve. The viscous stress tensor is [11]

$$\mathbb{T} = \mu(\nabla\mathbf{u} + (\nabla\mathbf{u})^T) - \frac{2}{3}\mu(\nabla\cdot\mathbf{u})\mathbf{u}. \tag{3}$$

Assuming also incompressibility, the continuity equation (2) reduces to the relation $\nabla\cdot\mathbf{u} = 0$. This leads to the vanishing of the last term in the viscous stress tensor and the cross-terms of the first part. Groundwater flow is also assumed stable, so the time dependence vanishes. The Navier-Stokes equations take the form

$$\rho(\mathbf{u}\cdot\nabla)\mathbf{u} = -\nabla p + \mu\nabla^2\mathbf{u} \tag{4}$$

and

$$\nabla\cdot\mathbf{u} = 0. \tag{5}$$

Since the flow velocities of groundwater are very small, the Reynolds number, $Re = \frac{\mathbf{u}L}{\nu}$, is significantly less than one and the flow is laminar. In this work, the Reynolds number is in fact low enough to make the assumption of Stokes' equation. The term on left-hand side of the momentum balance equation could be neglected.

A fracture is surrounded by the bedrock, which is assumed to be impermeable. Hence all the other walls than the fracture inlet and outlet are set with a no flux-boundary condition. The inlet holds a laminar inflow - condition, with a set average inflow. Pressure at the outlet boundary is set as zero.

2.2 Radionuclide transport in a fracture

The radionuclides dissolved into the groundwater in the bedrock fractures are transported by convection and diffusion. The diffusive migration of nuclides from higher concentration to lower concentrations is commonly described by Fick's law, and it is assumed to be valid in the fracture transport here. The governing equation of transport in water is the mass balance equation

$$\frac{\partial c}{\partial t} + \nabla \cdot \mathbf{J} = R, \tag{6}$$

where c is the concentration of the species, R a source or sink term and $\mathbf{J}$ the flux term

$$\mathbf{J} = \mathbf{J}_{\text{diff}} + \mathbf{J}_{\text{conv}} = -D\nabla c + \mathbf{u}c. \tag{7}$$

$\mathbf{u}$ is the velocity field and D the diffusion coefficient.

2.3 Matrix diffusion

Bedrock consist of a solid but porous rock matrix and larger fractures, which conduct the groundwater. Most of the transport of radionuclides takes place in the fractures, but diffusion of species to the rock matrix can happen. This effect is called matrix diffusion, and it is important because it increases the retention of radionuclides in the channel.

Rock matrix can be considered as a saturated porous medium, which consists of the solid rock matrix and pores saturated with water. The mass balance equation takes the form

$$\frac{\partial}{\partial t}\left(\varepsilon c_{\text{w}} + \rho_{\text{dry}} c_{\text{s}}\right) + \nabla \cdot \mathbf{J} + R = 0, \tag{8}$$

where ε is porosity, c_{w} concentration of the species in pore water (mol/m^3), c_{s} the mass content in the solid (mol/kg) and $\mathbf{J}$ the total flux of the species including diffusive and convective terms [10]. The first term describes the accumulation to the pore water and solid phase.

In the case of crystalline bedrock, the velocity of groundwater in the matrix can well be assumed to be zero, as the velocities are negligible compared to flow velocity in fractures. Thus we loose the convective part of the flux. Porosity and density are assumed to be constant. These simplifications lead to equation

$$\varepsilon \frac{\partial c_{\text{w}}}{\partial t} + \rho_{\text{dry}} \frac{\partial c_{\text{s}}}{\partial t} + \nabla \cdot \mathbf{J}_{\text{diff}} = 0, \tag{9}$$

where the source term is ignored.

The concentration in the solid is dependent on the concentration in pore water. Commonly, a linear equilibrium sorption model of the dependence is used $c_\mathrm{s} = K_\mathrm{d} c_\mathrm{w}$, where the parameter K_d is the volume-based distribution coefficient (m^3/kg) that must be determined experimentally [10]. Fick's law of diffusion is used for the flux term, where the effective diffusion coefficient can be determined experimentally. The equation can be written as

$$(\varepsilon + \rho_\mathrm{dry} K_\mathrm{d}) \frac{\partial c_\mathrm{w}}{\partial t} = \nabla \cdot (D_\mathrm{eff} \nabla c_\mathrm{w}) \,. \tag{10}$$

2.4 Formulation of the problem

The general structure consists of the fracture where flow occurs according to Navier-Stokes equations and the transport of radionuclides follows the transport equation (6). The fracture is surrounded by the rock matrix, where there is no convection, and transport occurs according to matrix diffusion equation. At the internal boundaries the velocity of water is zero and concentration is continuous across the boundary.

The mathematical formulation of the problem of the flow of water in the fracture is to find $\mathbf{u} = \mathbf{u}(\mathbf{x}) = (u(\mathbf{x}), v(\mathbf{x}), w(\mathbf{x}))$ and $p = p(\mathbf{x})$ such that

$$\begin{cases} \rho(\mathbf{u}\cdot\nabla)\mathbf{u} = -\nabla p + \mu \nabla^2 \mathbf{u} & \\ \nabla \cdot \mathbf{u} = 0 & \text{in } \Omega_\mathrm{fracture}, \end{cases} \tag{11}$$

with boundary conditions

$$\begin{aligned} p_\mathrm{entr} \cdot \mathbf{n} &= L_\mathrm{entr} \nabla \cdot \left[p_\mathrm{entr} \mathbf{I} + \mu(\nabla \mathbf{u} + (\nabla \mathbf{u})^T) \right], \ \nabla \cdot \mathbf{u} = 0 && \text{on } \partial\Omega_\mathrm{inlet} \\ p &= p_\mathrm{outlet} && \text{on } \partial\Omega_\mathrm{outlet} \\ \mathbf{u} \cdot \mathbf{n} &= 0 && \text{on } \partial\Omega_\mathrm{restoffrac}. \end{aligned} \tag{12}$$

At the inlet, an entrance region of length L_entr is assumed. p_entr is adjusted to give the desired average flow velocity or flow rate.

In the transport problem, the surrounding matrix domain must be finite in all directions. Hence, a no-flux boundary condition is set on all boundaries of the matrix, even to the rock matrix surrounding the inlet. This is physically unrealistic and may cause numerical problems. On fracture inlet boundary, an incoming concentration pulse $f(t)$ is defined. When $\mathbf{u}$ is solved, the mass transport problem is to find $c = c(\mathbf{x}, t)$ such that

$$\begin{cases} \dfrac{\partial c}{\partial t} + \nabla \cdot (-D \nabla c + \mathbf{u} c) = 0 & \text{in } \Omega_\mathrm{fracture} \\ (\varepsilon + \rho_\mathrm{dry} K_\mathrm{d}) \dfrac{\partial c}{\partial t} + \nabla \cdot (-D_\mathrm{eff} \nabla c) = 0 & \text{in } \Omega_\mathrm{rock} \end{cases} \tag{13}$$

with boundary conditions

$$
\begin{aligned}
c(\mathbf{x}, t) = f(t) &\quad \text{on } \partial\Omega_{\text{inlet}} \\
\mathbf{J}_{\text{diff}} \cdot \mathbf{n} = 0 &\quad \text{on } \partial\Omega_{\text{outlet}} \\
\mathbf{J} \cdot \mathbf{n} = 0 &\quad \text{on } \partial\Omega_{\text{rest}}
\end{aligned} \tag{14}
$$

and the initial condition $c(\mathbf{x}, t = 0) = 0$ in the entire geometry.

3 Methods

3.1 Fracture geometries

The creative problem in this assignment is to build credible, adequate and sufficiently realistic fracture planes. This problem is approached by considering the birth process of fractures. They are commonly created when an originally intact rock is divided in two, and thus the fracture has two similar opposing surfaces. After this division the aperture should be zero, but in reality the surfaces might have displaced in respect to each other, or some eroding processes might have taken place [12].

Normally, the walls of a fracture are in contact at several places, creating areas where the aperture is zero. A measured aperture distribution is approximately a gaussian shaped curve, plus a peak of points with zero aperture [12].

The fracture planes are created by making a random matrix from normal distribution. The planes were created with MATLAB software, using "randn"-function as the random number generator. It returns a normally distributed selection of random numbers, suitable to represent the aperture, and in line with the experimental results. The random matrix is smoothed using "medfilt2"-function in order to avoid numerically too steep gradients on the surface. It produces median filtering of a matrix. The function calculates the median of the neighbouring 3 by 3 entities.

Based on the experimental information on fracture topologies, the first modification from a smooth fracture is an irregular fracture that has two identical surfaces as walls at a distance from each other ("Even", figure 2). Thus the aperture remains constant through the fracture, but the surface area of the fracture plane is larger than that of a smooth fracture, increasing the tortuousity of the path.

The next model type has two similar random surfaces as top and bottom, but the aperture is not constant, but varies according to a sine function ("Narrow", figure 3). This modification creates narrower and wider aperture regions. The most complicated model type has a random aperture and both surfaces undulate based on a sine function, "Random" in figure 4.

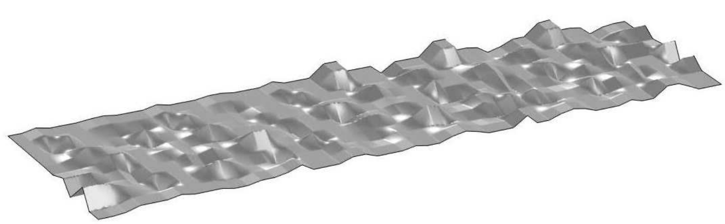

Figure 2: Fracture surface of model Even, with a constant aperture of 1 mm.

All fractures are 0.5 m long and 0.1 m wide. Planes created with Matlab are imported to COMSOL, where they generate parametric surfaces. A geometry is built so that the parametric surfaces form the top and bottom planes of the fracture. A block of solid rock is added to both sides of the fracture. The thickness of the rock layer

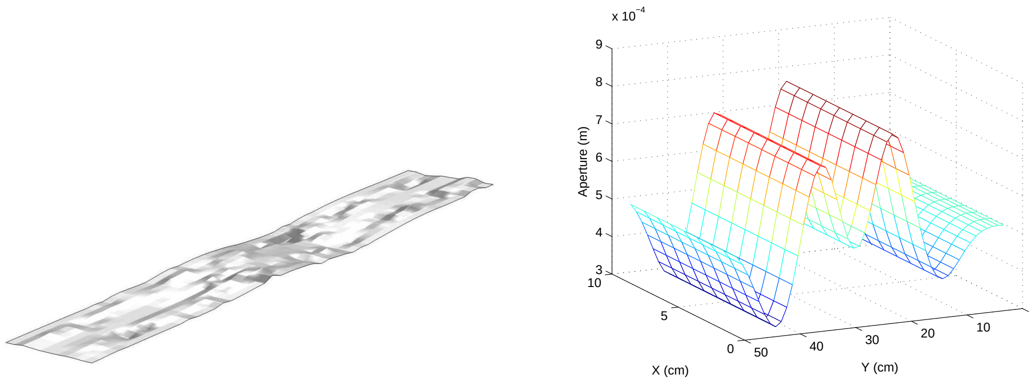

(a) Fracture surface.

(b) Aperture profile

Figure 3: The fracture surface and aperture profile of the model Narrow.

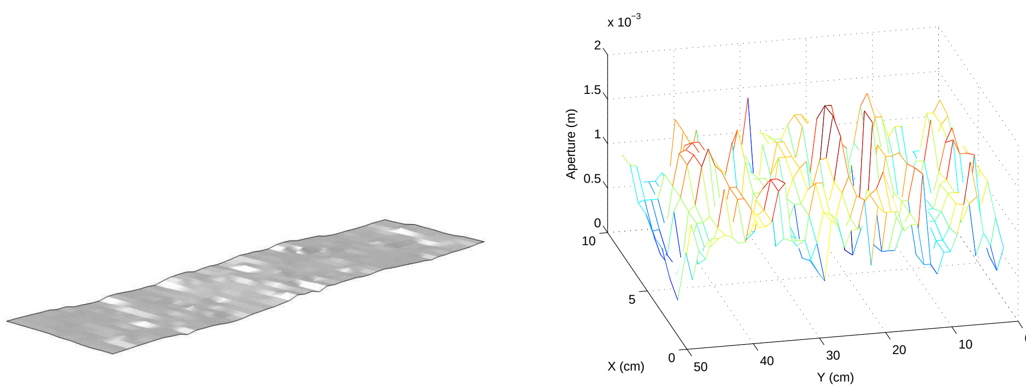

(a) Fracture surface.

(b) Aperture profile

Figure 4: The fracture surface and aperture profile of the model Random.

is varied according to the parameter K_d. As K_d increases, a thinner layer of rock participates in matrix diffusion, since the diffusion is retarded by nuclides attaching chemically to bedrock.

The three synthetic fracture models are studied in two cases. First, the average inflow velocity to the fracture remains constant and the models are solved with different values of parameter K_d. In the second case K_d is held constant as the inflow velocity is varied. The smooth-walled fracture is used as a reference case to which the other ones are compared. The peak of the release curve defines the transport time.

Surfaces can be classified based on their roughness, measured as area in respect to the smooth area. Fractures can be sorted based on their mean aperture and the standard deviation of the aperture. The so called coefficient of variation $CV = \sigma/\bar{b}$, where σ is the standard deviation and $\bar{b}$ is the mean aperture, is also often used in the comparison of fractures [12]. The descriptive parameters of the fractures are listed in the Table 1, as well as the calculated maximum flow velocities.

Table 1: Created fracture models and their statistical parameters.

Model	$\bar{b}$ (m)	σ (m)	CV	Surface/Smooth	v_{max} (m/s)
Smooth	$1.0 \cdot 10^{-3}$	0	0	1	$1.5 \cdot 10^{-9}$
Even	$1.0 \cdot 10^{-3}$	0	0	1.092	$2.7 \cdot 10^{-9}$
Narrow	$0.5 \cdot 10^{-3}$	$4.4 \cdot 10^{-12}$	$8.8 \cdot 10^{-9}$	1.017	$3.1 \cdot 10^{-9}$
Random	$1.0 \cdot 10^{-3}$	$4.2 \cdot 10^{-5}$	0.042	1.005	$4.5 \cdot 10^{-9}$

3.2 Computational tool - COMSOL Multiphysics

COMSOL Multiphsics solves partial differential equations with initial and boundary values numerically, by discretizing equations spatially using the Finite Element Method (FEM). This enables the solving of physical problems in complex geometries. Time dependent problems require also a time-discretization method, to which COMSOL offers either IDA [13] or Generalized-α [14].

There is a number of different types of finite elements to use to approximate the dependent variable at the mesh intervals, and the most simple case is to use linear elements. The linear functions are called the basis functions and they define the finite element space [15]. In this work, only linear and quadratic Lagrangian elements are used.

Numerical solutions to convection-diffusion equations can sometimes exhibit oscillations. The parameter that tells when a numerical problem becomes unstable is the Peclet number

$$Pe = \frac{\|\mathbf{u}\| h}{2 \cdot D} > 1, \tag{15}$$

where $\mathbf{u}$ is velocity, D the diffusion coefficient and h the mesh element size. Peclet's number measures the relative dominance between convection and diffusion. Oscillations occur most likely when the Peclet number condition applies and one of following conditions is true. Firstly, a Dirichlet boundary condition can lead to a steep gradient next to the boundary. With an unsuitable mesh, this leads to problems. Secondly, space dependent initial conditions can create local disturbances, which affect throughout the calculation. Thirdly, a small initial diffusion term close to a non-constant source term or boundary can result in a local disturbance. All these problems can be fixed by deforming and refining the mesh. However, this can lead to impractically dense meshes and thus to very long calculation times. Instead, stabilization methods are used. All stabilization methods add terms to the transport equation, which stabilize the calculation. The consistent stabilization methods used are the streamline upwind Petrov-Galerkin (SUPG) [15] and crosswind diffusion [16].

3.2.1 Fluid flow

Fluid flow is modelled with the Laminar Flow interface. It solves the Navier-Stokes equations (4) in the laminar case. In the case presented in this work, the flow field remains constant, and it can be solved as a stationary problem (Eq. 11). The nonlinear solver uses an affine invariant form of damped Newton method. The linear solver used to compute the linearised model is MUMPS (MUltifrontal Massively Parallel sparse direct Solver). The system is stabilized with both Streamline and Crosswind diffusion. Discretization of fluids is type P1 + P1, linear elements for both velocity and pressure, which requires significantly less memory and solves faster than P2 + P1, which uses second order elements for velocity components. Otherwise the default settings work sufficiently.

3.2.2 Species transport

Transport of radionuclides is modelled with Transport of Diluted Species interface. Another option would have been the Species Transport in Porous Media interface. The latter would in fact have been more suitable for this problem, since it solves equation 10, not Eq. 6 as the Diluted Species Interface. However, it has no built-in stabilization methods at all, which leads to relatively large negative concentrations, if applied without a very dense and memory-consuming mesh. The required changes to Transport of Diluted Species interface can be made directly to the equations COMSOL solves. Only the coefficients related to transport in porous media (Eq. 10) versus normal transport equations (Eq. 6) need to be added.

Transport phenomenon applies to the whole system, but different equations apply to the rock matrix than the fracture and hence the different settings. In fracture there is assumed to be no solid material, and the flowing fluid is water. In this domain Navier-Stokes equations Eq. (4) and transport equation Eq. (6) are solved. In the matrix on the other hand, the fluid is assumed to be stagnant, and matter is transported only by diffusion. In this domain the Navier-Stokes is not solved, and the transport equation must be modified to Eq. (10).

Due to the numerical difficulties that arise from the geometry, IDA is a better method for the time-discretization, since Generalized-α is less robust. IDA uses variable-order variable-step-size backward differentiation formula (BDF). The possibly non-linear system of equations is solved with Newton solver and the final linear system is solved with a suitable linear solver.

The steep incoming pulse at one boundary and the surrounding domains with a diffusion coefficient that differs many orders of magnitude, create some numerical problems. Negative concentrations can rise to match the positive concentrations. This makes a very dense mesh necessary, and in addition requires stabilization.

4 Results

The task is to calculate the travel time of radionuclides trough a fracture in four different fracture geometries. The travel time is defined as the time difference between the peaks of in and output pulses. The average inflow velocity U_{ave} and sorption parameter K_{d} are varied. First the model is validated comparing it to an analytical solution.

The required initial parameters are densities, fluid viscosity, porosity and diffusion coefficients. Density of water is assumed as normal water density, and viscosity $\mu =$ 0.01 Pa s. The value of viscosity is somewhat incorrect, but it has no effect on the velocity field with the current boundary conditions and low velocities [1]. The value for porosity is obtained from the simplified relation $\varepsilon = D_{\mathrm{eff}}/D_{\mathrm{w}}$, where the effective diffusion coefficient D_{eff} is determined experimentally [4]. The value of bulk density of bedrock is from Ref. [4]. Values can be found in Table 2. The incoming pulse of radionuclides is set as a Gaussian peak pulse, occurring during the first 1000 s, peaking at 8 mol/m^3, presented in figure 5.

Table 2: Used parameter values

ε_f	ρ_w	D_w	ε	ρ_b	D_{eff}
1	1000	$2{\cdot}10^{-9}$	$3{\cdot}10^{-5}$	2700	$6{\cdot}10^{-14}$
-	kg/m^3	m^2/s	-	kg/m^3	m^2/s

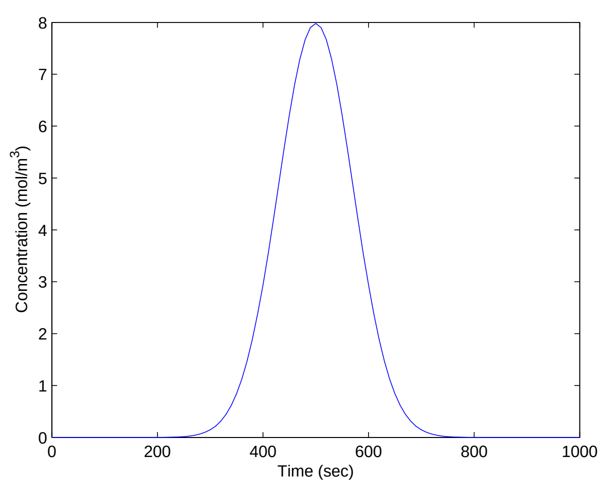

Figure 5: Incoming pulse.

[1] The very low velocities of the problem give a Reynolds number low enough to make the assumption of Stokes' equation. In Stokes' type problem with applied boundary conditions, viscosity has no effect on the resulting velocity field, it only scales the value of pressure. The wrong value of viscosity was unnoticed, and not corrected since it does not affect transport.

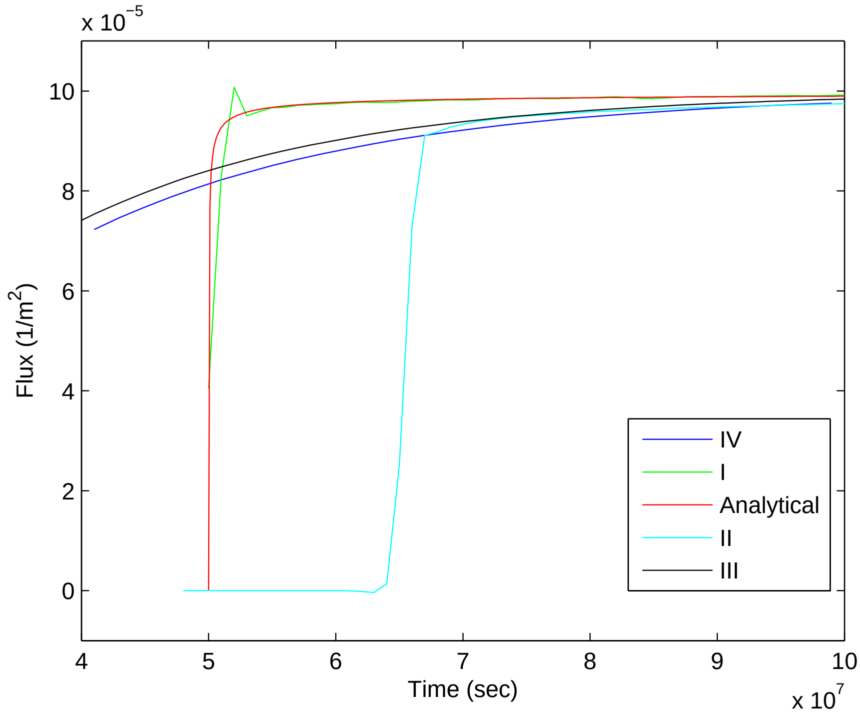

Figure 6: Release curves from a smooth fracture. I: constant flow-field and vertical diffusion, II: Navier-Stokes flow-field and vertical diffusion, III: constant flow-field and isotropic diffusion, IV: Navier-Stokes flow-field and isotropic diffusion, analytical solution.

4.1 Validation

The Graez problem of temperature diffusion in pressure-driven flow is often applied to convection/diffusion problems on particles [17]. A simplified solution for flow between parallel plates can be solved analytically. For a case of constant inflow, the shape of the release curve is of an error function [18, 19]

$$C_{\mathrm{f}}(L, t - t_{\mathrm{w}}) = C_0 \mathrm{erfc}(u t^{-1/2}), \tag{16}$$

where

$$u = [\varepsilon D_{\mathrm{eff}} R]^{1/2} \cdot \frac{WL}{Q}. \tag{17}$$

R is the retardation coefficient, which is 1 for a non-sorbing species and $R \approx K_{\mathrm{d}}\rho/\varepsilon$ for sorbing, W is the width of the channel, L the transport distance and Q the flow rate. This solution is obtained by making the assumptions of smooth fracture, constant velocity profile and diffusion only in z-direction. In order to validate the constructed COMSOL model, such a simplified case is solved first. Next, the model will be complicated in two separate steps: First the velocity field is solved with Navier-Stokes equations keeping diffusion vertical, and second, the transport equation is solved with isotropic diffusion, keeping the flow field constant. The release curves are compared to the analytical solution. Finally, a version with both

Navier-Stokes-flow field and isotropic diffusion is solved; similar approach is used in the actual models.

From figure 6 can be seen, that the first COMSOL solution for the most simplified case is the same as the analytical, apart from some numerical oscillation. Adding isotropic diffusion makes a very significant difference to the shape of the curve. In the isotropic case the release starts at one order of magnitude earlier. Changing from constant velocity field to Navier-Stokes keeps the shape of the curve sharp, but the peak occurs later.

4.2 Varying K_d

Four models were solved with three different values of K_d: 0, 10^{-3} m^3/kg, 10^{-1} m^3/kg. Measured coefficients for many interesting radionuclides are within these limits [19]. Simulations with larger K_d:s are less significant, due to very long travel times induced by strong retention. When K_d is set to zero the rock matrix is 50 cm thick on both sides. This distance was chosen since it was large enough to limit the numerical effects of the walls of the bedrock domain, and was still reasonable to mesh. With larger values of K_d the distance is 3-5 cm, which is enough because of the stronger retention. The calculated transport times through the fractures are listed in table 3. All models have the same average inlet velocity of 10^{-9} m/s.

Table 3: Transport times when varying K_d, $U_\mathrm{ave} = 10^{-9}$ m/s.

K_d (m^3/kg)	0	10^{-3}	10^{-1}
		T (s)	
Smooth	$2.0{\cdot}10^7$	$4.6{\cdot}10^7$	$2.4{\cdot}10^9$
Even	$2.2{\cdot}10^7$	$7.3{\cdot}10^7$	$5.1{\cdot}10^9$
Narrow	$2.1{\cdot}10^7$	$12{\cdot}10^7$	$10{\cdot}10^9$
Random	$2.0{\cdot}10^7$	$4.6{\cdot}10^7$	$3.0{\cdot}10^9$

As seen from the results, the order of the models is quite clear. Narrow is always the slowest and Even second to last, except the case when $K_\mathrm{d} = 0$. Smooth and Random give approximately same values, except for the case $K_\mathrm{d} = 10^{-1}$, when Smooth is the fastest.

The solution obtained in the fracture is very smooth. In the bedrock, area close to the entrance exhibits some oscillation. This is most likely due to the geometry, where the sharp inflow pulse and no-flow boundary condition areas are next to each other. The effect can be seen in figure 8, close to the entrance of the fracture. The solution is smooth in the bedrock further along the channel.

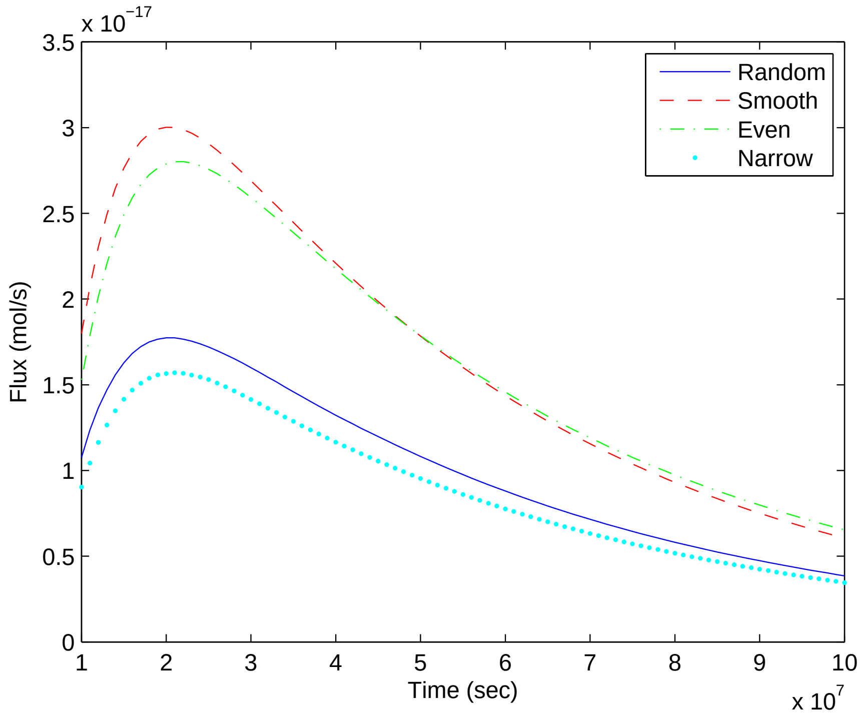

Figure 7: Release curves from the fractures, $K_{\mathrm{d}} = 0$, $U_{\mathrm{ave}} = 10^{-9}$ m/s.

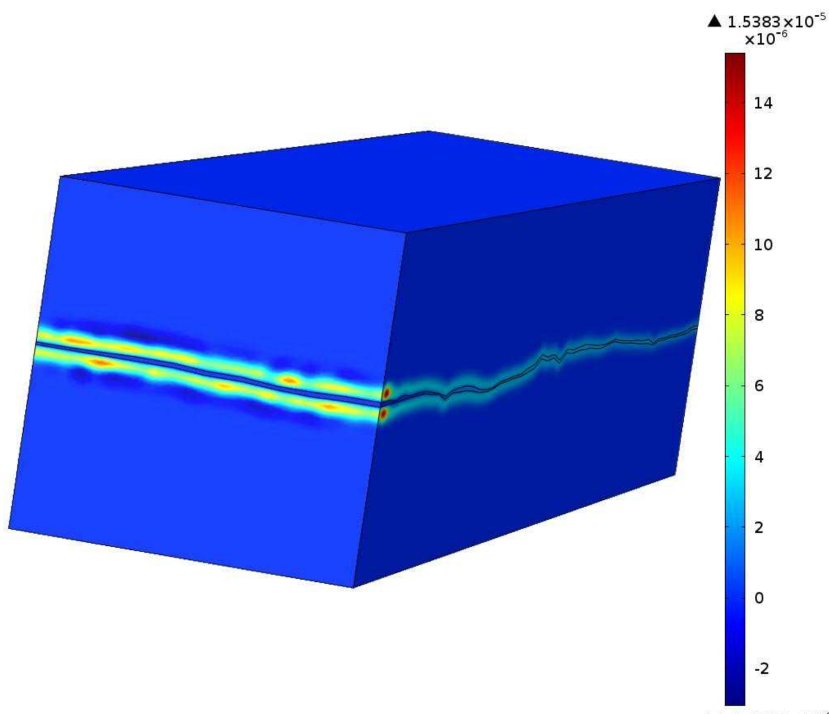

Figure 8: Concentration oscillations above the entrance of the fracture of model Random, seen as red and dark areas at the entrance head (left surface in the picture).

4.3 Varying average flow velocity

In this case the sorption parameter K_d remains at constant value 10^{-3}. The average flow velocity in the fracture is varied. It is increased from 10^{-9} m/s to 10^{-8} m/s, 10^{-7} m/s and 10^{-6} m/s. The calculated transport times are listed in Table 4. The slowest model is in every case Narrow. From the 1 mm thick models, Even is always the slowest and Random and Smooth almost equal.

From the results it can be seen, that the decrease in transport time is greater at faster velocities. The last step from 10^{-7} to 10^{-6} holds the greatest difference. The order of magnitude change in velocity transfers fully to transport time. When the average velocity is decreased, the transport time does not grow as much, and the transport times are closer to each other.

The shape of release curve transforms when changing the velocity. In the fastest case a sharp spike with a long low tail forms. This can be seen when comparing for example the figures 10 and 12, which present release curves at average velocities of 10^{-8} and 10^{-6} respectively.

Table 4: Transport times when varying the average inflow velocity, $K_d = 10^{-3}$ m^3/kg.

U_{ave} (m/s)	10^{-9}	10^{-8}	10^{-7}	10^{-6}
		T (s)		
Smooth	$4.6 \cdot 10^7$	$3.8 \cdot 10^7$	$0.94 \cdot 10^7$	$1.1 \cdot 10^6$
Even	$7.3 \cdot 10^7$	$4.7 \cdot 10^7$	$1.3 \cdot 10^7$	$1.4 \cdot 10^6$
Narrow	$12 \cdot 10^7$	$10 \cdot 10^7$	$2.1 \cdot 10^7$	$2.1 \cdot 10^6$
Random	$4.6 \cdot 10^7$	$3.9 \cdot 10^7$	$0.94 \cdot 10^7$	$1.0 \cdot 10^6$

Between the models in figures 9 and 10, Smooth has clearly a steeper peak that rises higher and decreases faster than the other ones. Random and Even peak approximately equally high, but Even reaches the peak slightly later and Random decreases faster. The release curve of Narrow starts only at 10^8 s and is lower and flatter and does not fit into the pictures.

In figures 11 and 12 similar behaviour is seen. Smooth peaks higher, Random and Even peak quite close to each other, Even a bit later. Narrow forms a much lower and wider pulse, that occurs a lot later. In figure 11 Random is higher than Even and narrower than the other models. In 12 Smooth has a significantly narrower peak than the others. The pulses are very distinct and all models have long and very low tails.

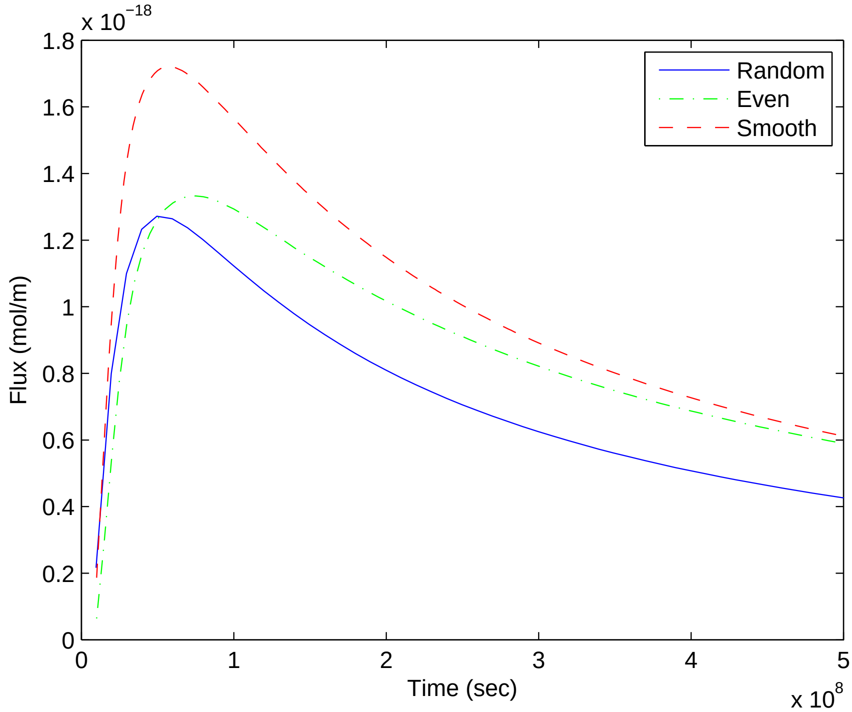

Figure 9: Release curves of models Smooth, Random and Even, $U_{\mathrm{ave}} = 10^{-9}$ m/s, $K_{\mathrm{d}} = 10^{-3}$ m^3/kg.

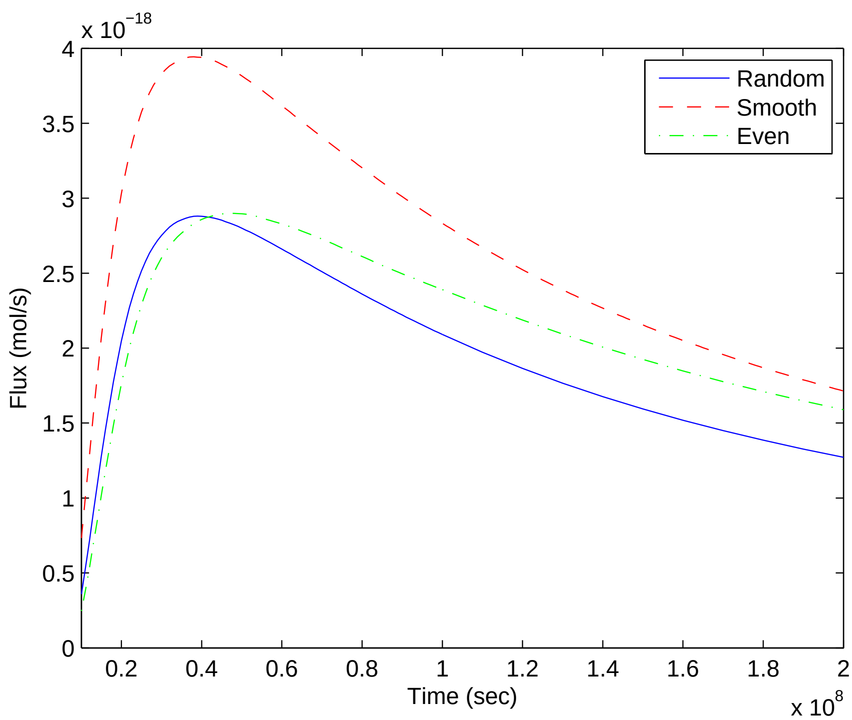

Figure 10: Release curves of models Smooth, Random and Even, $U_{\mathrm{ave}} = 10^{-8}$ m/s, $K_{\mathrm{d}} = 10^{-3}$ m^3/kg.

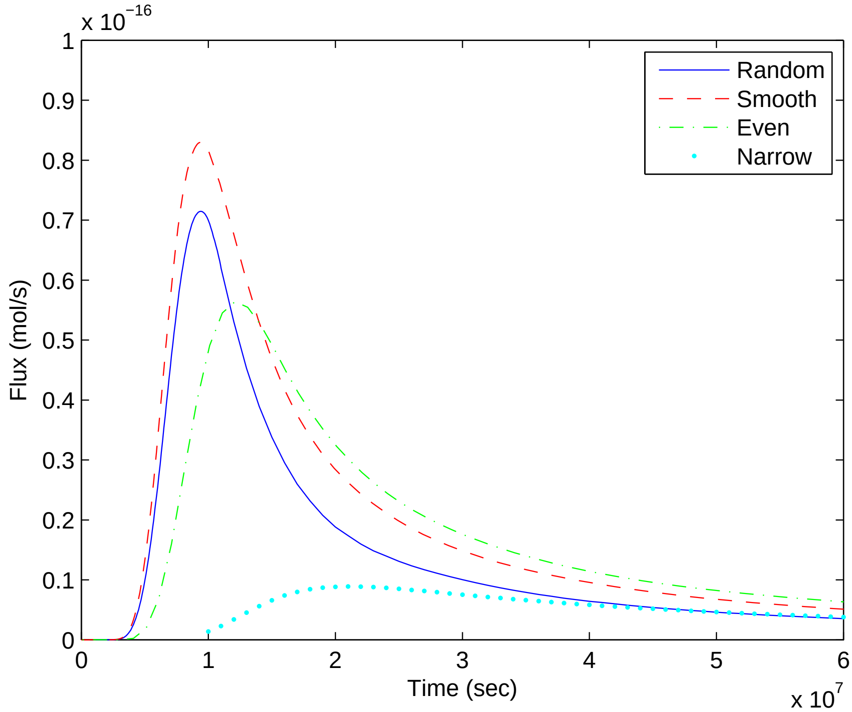

Figure 11: Release curves of models Smooth, Random, Even and Narrow, $U_{\mathrm{ave}} = 10^{-7}$ m/s, $K_{\mathrm{d}} = 10^{-3}$ m^3/kg.

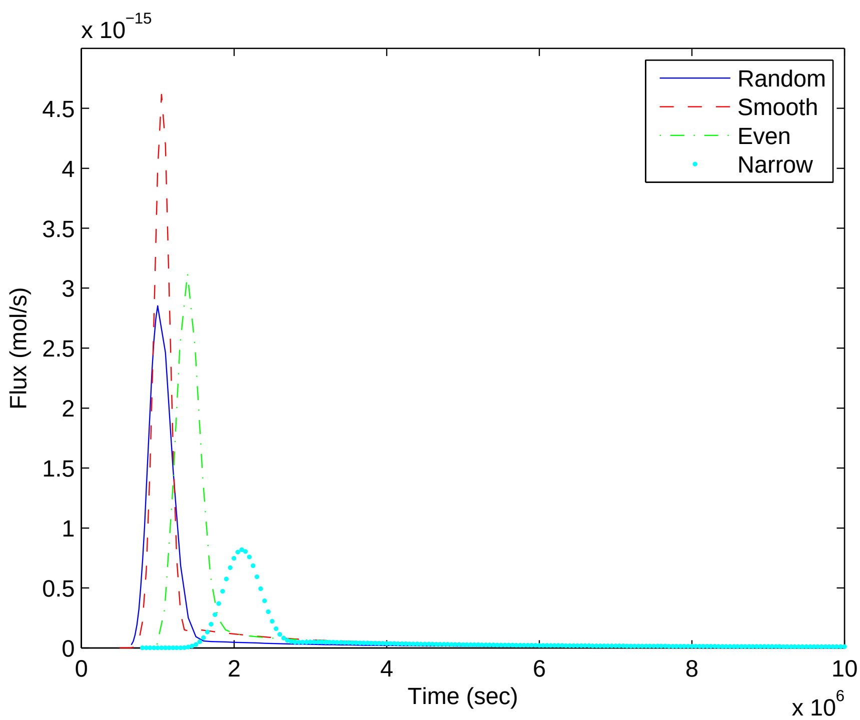

Figure 12: Release curves of models Smooth, Random, Even and Narrow, $U_{\mathrm{ave}} = 10^{-6}$ m/s, $K_{\mathrm{d}} = 10^{-3}$ m^3/kg.

5 Discussion

The model seems to be sufficiently well constructed since the validation is successful. The validation shows that the used additions to the model, non-constant flow field and isotropic molecular diffusion, change the shape of the solution significantly (figure 6). Diffusion induces the greatest change. Navier-Stokes flow field does not change the shape of the release curve in a smooth fracture.

Increasing the sorption parameter K_d increases the differences of transport time between the models. At $K_\mathrm{d} = 0$, the transport times are almost the same and very short, approximately $2 \cdot 10^7$ seconds (Table 3). The approximate travel time of the water through the fracture, calculated at constant speed 10^{-9} m/s is $5 \cdot 10^8$ s. This is more than an order of magnitude longer than the calculated travel times for radionuclides. The effect of longitudinal diffusion is the most likely explanation, since with this low velocity of water, diffusion is large compared to convection. Diffusion as an important transport mechanism would also explain why the models give practically the same result. Their velocity profiles might vary, but all have the same diffusion coefficient in water.

The importance of molecular diffusion becomes significant when the diffusion coefficient is close to the same order of magnitude as the flow velocity. From Table 4 can be noticed, that increasing the velocity increases the differences between models, and the transport times are closer to the transport times of water. The shape of the release curves also show this effect by loosing the smoothing effect of diffusion at greater speeds. In figures 9 and 10 the release curves are still very similar and the maximum flux is the same order of magnitude in them both. When the flow is fast enough, the dispersion decreases radically, the shapes of the release curves are much clearer in figure 11, which still contains large diffusion induced tails. In figure 12, where the original inflow pulse has changed shape only marginally.

When K_d is increased to 10^{-3}, the travel times increase compared to no retention, and differences between models increase, as is seen in Table 3. The surface area plays a more important part, as it increases the retention. The transport times are still faster than the average water transport time, which indicates that diffusion is still important. It takes retention as strong as $K_\mathrm{d} = 10^{-1}$ to the transport times to reach the order of magnitude of water transport time.

The models Smooth and Random have transport times very close to each other at $K_\mathrm{d} = 10^{-3}$, but the release peak of Random is lower and wider. This is due to dispersion in the randomly shaped fracture. It seems that the faster transport regions compensate to the larger surface area and narrow regions, so that it transports as fast as Smooth. Increasing the flow velocity effects Random at first, which can be seen from the higher and narrower release pulse in figure 11. When K_d is increased to 10^{-1}, Smooth is the fastest model, and Random is left behind, due to the greater surface area.

At $K_\mathrm{d} = 0$, Even is very close to Smooth in both transport time and height of pulse. It would seem that when there is no retention, the aperture variances lower the release curves of the other two. When retention is added, the height of the peak of Even decreases significantly, close to the height of Random. The transport time of Even also slows down, when the retention is increased. Even has much greater surface area than the others, which is the reason for these effects.

Narrow is by far the slowest model when retention is included. It has half the average aperture of the others, and an even narrower region perpendicular to the direction of the flow to transport through (figure 3(b)). Longer transport time means more dispersion, which can be seen from the much wider retention curves of Narrow in figure 12. At $K_\mathrm{d} = 0$ though, it transports just like the other models, figure 7, creating only slightly lower and wider release curve as Random.

6 Conclusions

Based on this study, it would seem that the parallel plate fracture is not a good approximation for all kinds of fractures. Fortunately, mostly the results show that the simplified case underestimates the transport time through fractures. This is in line with the conservative principle used in safety assessment that tends to exaggerate to the pessimistic side. In the model with largest standard deviation and greatest maximum velocity, the transport time was around the same as in the smooth fracture, at specific parameter values.

Fractures with significant standard deviations were not created, since the meshing turned out to be very difficult. None of the models has a fracture with an optimal geometry for strong channelling either. Based on this study, it cannot be said that the pulse might transmit through faster than in the smooth case. More study in the field of large variance fractures is needed to fully evaluate the effect. Also, a broader take of parameters and their combinations would give a lot more insight to the problem. The varying of average velocity could be carried out with more values of K_d, and varying of K_d with different velocities. Especially simulations with faster velocities would bring more information, since the diffusion is very strong at most of the velocities examined in this work. Solving more combinations would have been too extensive to the scope of this work.

Another notice was that adding isotropic diffusion smooths and fastens the output pulses significantly, when the flow velocity is low enough. Differences of travel time between models decrease prominently and the form of the release curve changes too. The sharp, high output pulse of high velocities transforms to a low and very slowly decreasing curve, as the flow velocity and diffusion coefficient reach a suitable ratio. Diffusion has an effect to almost all cases presented, but the main features of the results can still be seen.

The modelling of transport in a rough fracture with FEM type discretization proved to have some difficulties. The fractures modelled in this work had a very small coefficient of variation CV, as is seen in Table 1. Measured real fractures can easily have a CV of an order of magnitude larger. The large variance fractures proved to be difficult or impossible to mesh, and calculations with the resulting dense meshes are very memory-consuming. Also, the ratio of surface compared to the smooth surface remains very small, since it was not possible to create surfaces that resemble the fractal nature of natural fractures.

References

[1] K. Rasilainen and S. Vuori. Käytetyn ydinpolttoaineen huolto: suomalaisen suunnitelman pääpiirteet. *VTT TIEDOTTEITA: 1953*, 1999.

[2] M. Bunn, S. Fetter, J.P. Holdren, and B. Van Der Zwaan. The economics of reprocessing vs. direct disposal of spent nuclear fuel. *Project on Managing the Atom, Belfer Center for Science and International Affairs, John F. Kennedy School of Government, Harvard University*, 2003.

[3] Posiva Oy Official website. `http://www.posiva.fi/`, cited 18.4.2012.

[4] M. Nykyri, H. Nordman, N. Marcos, J. Löfman, A. Poteri, and A. Hautojärvi. Radionuclide release and transport–RNT-2008. *Posiva Report*, 6:170, 2008.

[5] K. Rasilainen and S. Vuori. Käytetyn ydinpolttoaineen huolto: turvallisuuden arvioinnin perusteet. *VTT TIEDOTTEITA: 2033*, 1999.

[6] M. Olin, K. Rasilainen, A. Itälä, V.M. Pulkkanen, M. Matusewicz, M. Tanhua-Tyrkkö, A. Muurinen, L. Ahonen, M. Kataja, P. Kekäläinen, et al. Bentoniittipuskurin kytketty käyttäytyminen. *Puskuri-hankkeen tuloksia*, 2011.

[7] A. Poteri. Retention properties of flow paths in fractured rock. *Hydrogeology Journal*, 17(5):1081–1092, 2009.

[8] C. Grenier, G. Bernard-Michel, and H. Benabderrahmane. Evaluation of retention properties of a semi-synthetic fractured block from modelling at performance assessment time scales (Äspö Hard Rock Laboratory, Sweden). *Hydrogeology Journal*, 17(5):1051–1066, 2009.

[9] J. Bodin, F. Delay, and G. De Marsily. Solute transport in a single fracture with negligible matrix permeability: 1. fundamental mechanisms. *Hydrogeology journal*, 11(4):418–433, 2003.

[10] J. Bodin, F. Delay, and G. De Marsily. Solute transport in a single fracture with negligible matrix permeability: 2. mathematical formalism. *Hydrogeology Journal*, 11(4):434–454, 2003.

[11] A.L. Fetter and J.D. Walecka. *Theoretical mechanics of particles and continua*. Dover Pubns, 2003.

[12] E. Hakami. *Aperture distribution of rock fractures*. PhD thesis, Royal Institute of Technology, 1995.

[13] A.C. Hindmarsh, P.N. Brown, K.E. Grant, S.I. Lee, R. Serban, D.E. Shumaker, and C.S. Woodwars. Sundials: Suite of nonlinear and differential/algebraic equation solvers. *ACM T. Math.Software*, 31:363, 2005.

[14] J. Chung and G.M. Hulbert. A time integration algorithm for structural dynamics with improved numerical dissipation: The generalized-α method. *J. Appl. Mech.*, 60:371–375, 1993.

[15] C Johnson. *Numerical Solution of Partial Differential Equations by the Finite Element Method*. Dover Pubns, 2009.

[16] V. John and P. Knobloch. On spurious oscillations at layers diminishing (SOLD) methods for convection–diffusion equations: Part i–a review. *Computer methods in applied mechanics and engineering*, 196(17):2197–2215, 2007.

[17] T. Gervais and K.F. Jensen. Mass transport and surface reactions in microfluidic systems. *Chemical engineering science*, 61(4):1102–1121, 2006.

[18] T. Vieno, H. Nordman, A. Poteri, F.A. Hautojärvi, and J. Vira. The Posiva/VTT approach to simplification of geosphere-transport models, and the role and assessment of conservatism. In *Confidence in models of radionuclide transport for site-specific assessments: Workshop proceedings, Carlsbad, New Mexico, United States, 14-17 June 1999*, page 119. Agence pour l'Energie Nucléaire, 2001.

[19] T. Vieno, Hautojärvi A., L. Koskinen, and H. Nordman. Käytetyn ydinpolttoaineen loppusijoituksen turvallisuusanalyysi TVO-92. *Nuclear Waste Commission of Finnish Power Companies*, 1992.

Series title and number
VTT Technology 128

Title	**The effect of geometry on radionuclide transport in a bedrock fracture**
Author(s)	Karita Kajanto
Abstract	a) Background b) What should be done? c) Methods and tool a) Estimating the long term safety of a geological nuclear waste repository is a complicated computational problem. Numerous scenarios of system failure must be taken into account. Released radionuclides can be transported long distances along the groundwater of rock fractures. Sorption into the bedrock may also take place. In the case of a release of radionuclides to the groundwater, transport properties in fractures must be well known. A common approximation of rock fracture flow is flow between parallel plates. The shape of natural fractures, however, is uneven and irregular. Varying shape and size causes dispersion that affects transport. b) Study the effect of dispersion caused by variable aperture fractures to the transport and flow properties. Build models of a single rock fracture in different credible geometries. Calculate the flow field and transport of a pulse of radionuclides trough the fractures. Also, calculate the retention of nuclides caused by matrix diffusion. Compare the results to the parallelplate case. c) Numerical methods: FEM with time integration. COMSOL Multiphysics 4.2a, CAD Import Module, Subsurface Flow Module, Chemical Reaction Engineering Module.
ISBN, ISSN	ISBN 978-951-38-8055-2 (URL: http://www.vtt.fi/publications/index.jsp) ISSN-L 2242-1211 ISSN 2242-122X (Online)
Date	September 2013
Language	English
Pages	29 p.
Name of the project	
Commissioned by	
Keywords	Radionuclide transport, bedrock fracture, matrix diffusion, parallel plate approximation
Publisher	VTT Technical Research Centre of Finland P.O. Box 1000, FI-02044 VTT, Finland, Tel. 020 722 111

The effect of geometry on radionuclide transport in a bedrock fracture

VTT TECHNOLOGY 128 The effect of geometry on radionuclide transport in a bedrock fracture

ISBN 978-951-38-8055-2 (URL: http://www.vtt.fi/publications/index.jsp)
ISSN-L 2242-1211
ISSN 2242-122X (Online)